ASIAN JOURNAL OF CIVIL ENGINEERING (BUILDING AND HOUSING) VOL. 7, NO. 3 (2006)
PAGES 213-224

FLEXURAL STIFFNESS DETERMINATION USING MODE SHAPE DERIVATIVE

H. Abdul Razak* and Z. Ismail
Department of Civil Engineering, University of Malaya,
50603 Kuala Lumpur, Malaysia

ABSTRACT

Flexural stiffness of a single load-induced crack is determined. Modal analysis is performed on the beam prior and after each load stage. Mode shapes are extracted and eigenvectors used to determine the mode shape equations. Global flexural stiffness is derived by utilizing the regressed variable λ and the local flexural stiffness is derived by applying the centered-finite-divided-difference formula on the regressed data. The global stiffness decreases with increasing severity of the crack. Results compared with values computed using the load-deflection plot showed similar trends. The algorithm may be used as a technique for detecting crack damage in reinforced concrete.

Keywords: flexural stiffness; rc beam; single crack; modal testing; mode shape; load-induced

1. INTRODUCTION

Conventional procedures for structural condition monitoring usually rely on visual inspection and are location-dependent. This study proposes the application of experimental modal analysis to evaluate the stiffness of reinforced concrete beams with cracks. The presence of a crack causes localized changes to flexural stiffness which is dependent on the severity of the crack.

There have been several significant investigations carried out to determine the existence and the severity of defects in structures using one or more of their modal properties [1-10]. In most of the dynamic tests conducted on actual structures the fundamental natural frequencies have been utilized and found to be the most convenient parameter to be studied [11,12]. It was found that the most easily observable change is the reduction in natural frequencies, and most investigators use this feature in one way or another [13-16].

Casas proposed a method of surveillance of concrete structures through monitoring the characteristics of the natural frequencies and mode shapes [17]. Varying success has been reported where the change in modal damping has been utilized, while some work has been

* Email-address of the corresponding author: hashim@um.edu.my

reported on the use of change of mode shape to detect damage [18].

West presented a systematic use of mode shape data in the location of structural damage without the use of a prior finite element model. The modal assurance criteria (MAC) was used to determine the level of correlation between modes from the test of an undamaged body flap and the modes from the test of the flap after it had been exposed to loading. The mode shapes were partitioned using various schemes, and the change in MAC across the different partitioning techniques was used to locate the structural damage [19]. Fox showed that shape changes such as the MAC are relatively insensitive to damage in a beam with a saw cut. Graphical comparisons of relative changes in mode shapes were shown to be the best way of detecting the damage location when only resonant frequencies and mode shapes were examined. A method of scaling the relative changes in mode shape to improve the process of identifying the location of the damage was also presented [20].

Ratcliffe presented a technique for locating damage in a beam that uses a finite difference approximation of a Laplacian operator on mode shape data. In the case of a damage which is not so severe, further processing of the Laplacian output is necessary before damage location could be determined. The procedure is found to be best suited for the mode shape obtained from fundamental natural frequency. The mode shapes obtained from higher natural frequencies may be used to verify the damage location, but they are not as sensitive as the lower modes [21].

An alternative method to using mode shapes in obtaining spatial information about sources of vibration changes is by using the mode shape derivatives, such as curvature. It is noted that for beams, plates, and shells there is a direct relationship between curvature and bending strain. Pandey, et al. demonstrated that absolute changes in mode shape curvature can be a good indicator of damage for the cantilever and simply supported analytical beam structures which they considered. The changes in the curvature increase with increase in damage. The curvature values were computed from the displacement mode shape using the central difference approximation [22].

Stubbs, et al. presented a method based on the decrease in the curvature of the measured mode shapes or the modal strain energy between two structural degrees of freedom [23]. Topole and Stubbs further showed that using a limited set of modal parameters for structural damage detection was feasible [24, 25]. Stubbs and Kim also showed that localizing damage using this technique without baseline modal parameters was also possible [26]. This approach was confirmed by Chance, et al. who found that numerically calculating curvature from mode shapes resulted in unacceptable errors. As a consequence measured strains were instead used to measure curvature directly, and this improved results significantly [27].

Shahrivar and Bouwkamp who presented the finite element and experimental data for a scale model of an offshore platform and found that the fundamental mode shape was more sensitive to damage than the fundamental vibration frequency, further confirm the sensitivity of the mode-shape method [28].

2. METHODOLOGY

In order to reduce the complexity of the equations of motion, the test beams was

approximated to behave as a Bernoulli-Euler beam. The beam parameter was approximately 1/9. This ratio could be smaller to reduce the effect of shear and to better approximate the Bernoulli-Euler beam as commented by Altay and Dokmeci [29]. According to Timoshenko et al. (1974) corrections to reduce the effect of shear is only necessary at higher frequencies. At lower frequencies like the cases for the research beams this effect is not significant.

The transverse forced vibration of such a beam is derived from Newton's Law of Motion and can be represented by

$$\frac{\partial^2}{\partial x^2}\left(EI\frac{\partial^2 v}{\partial x^2}\right)+\rho A\frac{\partial^2 v}{\partial t^2}=p(x,t) \tag{1}$$

For the case of free vibration this equation reduces to:

$$\frac{d^4 v}{dx^2}-\lambda^4 v=0 \tag{2}$$

where

$$\lambda^4=\frac{(\rho A\omega^2)}{EI} \tag{3}$$

The general solution of Eq. (2) may be written in the form

$$v(x)=C_1\sinh\lambda x+C_2\cosh\lambda x+C_3\sin\lambda x+C_4\lambda x \tag{4}$$

It was approximated that the generalized solution still applies for the beams with cracks assuming that the system remained continuous despite the presence of the cracks.

In this study, natural frequencies and mode shapes were obtained from modal testing. The mode shape data derived had discrete values, and an equation to represent these discrete values was required. The data were thus curve-fitted into the generalized mode shape equation (Eq. 4) by the least-squares regression method, which produced estimates for the unknown coefficients. The aim of this approach was to derive a single curve that represented the general trend of the data. A nonlinear regression technique, namely the Marquardt-Levenberg algorithm was used in this study for the curve fitting. It is a weighted average of Newton's method and the Steepest Descent method for nonlinear systems of equations [30, 31].

From the regressed mode shape data obtained above, the *global flexural stiffness* was obtained by using the estimated λ and rearranging Eq. (3). To obtain the local flexural stiffness, Eqn 2 was used in association with the finite difference applied to the regressed mode shape. A *normalized shape indicator EI* was thus obtained at each coordinate point again by rearranging Eq. (3).

For comparison, the RC beams were load tested by applying a point load at point 0.5*L* and 0.7*L*. In the load test, the applied load and deflection were measured during loading. The gradient of the linear portion of the load versus deflection plot gave the bending

characteristic of the test beams. Subsequently, the flexural stiffness of the beam was calculated from the load-deflection plot.

Using the theoretical mid-span deflections of a simply supported beam under point load, at mid span and a point L - b , where $b < 0.5L$, the bending stiffness of the beam, EI, could be calculated as $\mathrm{EI} = \left(\frac{\mathrm{L}^3}{48}\right)\left(\frac{\mathrm{P}}{\delta}\right)$ or $\mathrm{EI} = \left(\frac{\mathrm{b}(3\mathrm{L}^2 - 4\mathrm{b}^2}{48}\right)\left(\frac{\mathrm{P}}{\delta}\right)$ where (P/δ) is the gradient of the load versus deflection plot.

3. EXPERIMENTAL PROCEDURE

In this investigation, three RC beams were cast. The dimensions of the reinforced concrete beams were 150 mm wide and 250 mm deep. The beams were designed according to BS 8110, and the dimensions were such that they were as close as possible to full-scale beams within the constraints limited by difficulties with placing the reinforcement bars; at the same time having a suitable ultimate load. They were reinforced with three 10mm diameter high-yield bars with stirrups, and concrete cover of 25mm was provided. Figure 1 shows the cross sectional details of the test beams. The beams were simply supported across an effective span of 2200 mm on concrete blocks. The first beam had a crack at $0.5L$ and the second beam had a crack at $0.7L$. The third beam was the control beam, and modal testing was also carried out for this beam.

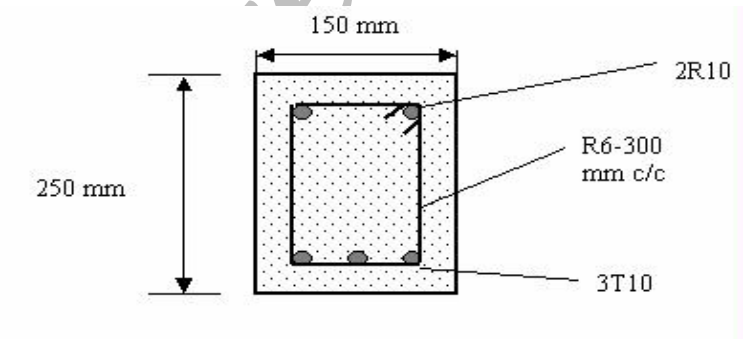

Figure 1. Details of the cross section of the test beams

The concrete for the test beams were designed in accordance to DOE method for grade 40 with 150 mm slump to give the desired workability. The mix proportion of the test beams is given in Table 1. Ordinary Portland cement (OPC), mining sand, and granite stone were used for cement, fine aggregates, and coarse aggregates, respectively. Water from the pipe supply was utilized as mixing water and water/cement ratio (w/c) was 0.45. All mix ingredients were obtained from the same brand and same batch in order to ensure the quality and uniformity in the test beams.

Table 1. The mix proportion of the test beams

Mix Properties (per cubic metre)	Weight (kg)	Percent (%)
Ordinary Portland Cement	380	17.5
Fine aggregate	750	34.5
Coarse aggregate (20mm)	880	40.5
Water	163	7.5
Total	2173	100
Water/Cement ratio (W/C)	0.43	
Superplasticizer R 1000	1.2 liter/100kg of cement	
Retarder P300 N	0.2 litre /100 kg of cement	

A 20 mm deep saw-cut was introduced at the corresponding soffit point across each of the beam. A concentrated point load was then applied at the position where the saw-cut was located. A load cycle was applied incrementally in the following manner: zero to maximum loading at increments of approximately 0.75 kN each time, and maximum loading to 0 kN with decrements of approximately 0.75 kN each time. Figure 2 depicts the set-up for static loading test. The first beam was subjected to maximum loading of 25 kN and 43 kN and modal testing carried out at each cycle while the second beam was subjected to maximum loading of 25, 41, 43, and 46 kN and again modal testing was carried out at each cycle. Crack widths, crack depths, and modal parameters were recorded for both beams at all cycles. Measurements for crack width of both beams were recorded from both sides of the beams at level 230mm from the top surface of the beams by using two crack gauges. Figure 3 shows how the crack widths were measured and the characteristics of the loading stages are summarized in Appendix A.

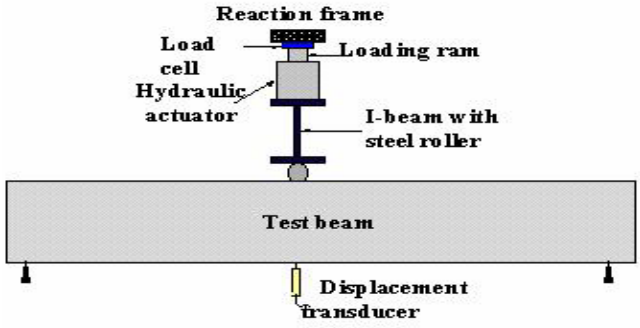

Figure 2. Static load test set-up

Figure 3. Measuring the crack width

3.1 Modal Test

Modal test was performed using transfer function technique on the RC beams, which were simply supported on concrete blocks. An accelerometer was used to pick up the response of the test beam under forced excitation. The excitation resulting from the input force was measured using a force transducer. The RC beams were randomly excited using white noise signal input to a shaker, which was permanently placed at the quarter span for all test beams. The accelerometer was moved from one coordinate point to another to pick up a total of fifty-six response signals along the length of the beam. The transfer functions were acquired through a signal analyser. Initially, the transfer function spectrum within a 5 kHz frequency span was obtained in order to locate roughly the resonant frequency peaks of all the flexural modes within the band. Subsequently, zooming within a 100Hz span of the resonant frequency peak of a particular mode was carried out. The measurements were made using a block size of 400 lines thus giving a resolution of 0.25Hz per spectral line.

A dual-channel analyzer was used to acquire the signals and to obtain the frequency response functions (FRF) from the response and the excitation force. By using modal analysis software, the curve fitting process was performed on the transfer function spectrums obtained to extract the modal parameters i.e. natural frequency, mode shape and damping. A total of ten normal bending modes were acquired in this manner. Figure 4 depicts the set-up of the modal testing.

4. RESULTS AND DISCUSSION

Appendix B lists the history of stiffness determination for beam with a crack at 0.5L and 0.7L.

The overall results showed that there were no discontinuities at the crack locations confirming that the assumption of the system remaining continuous over the experimental conditions were justified.

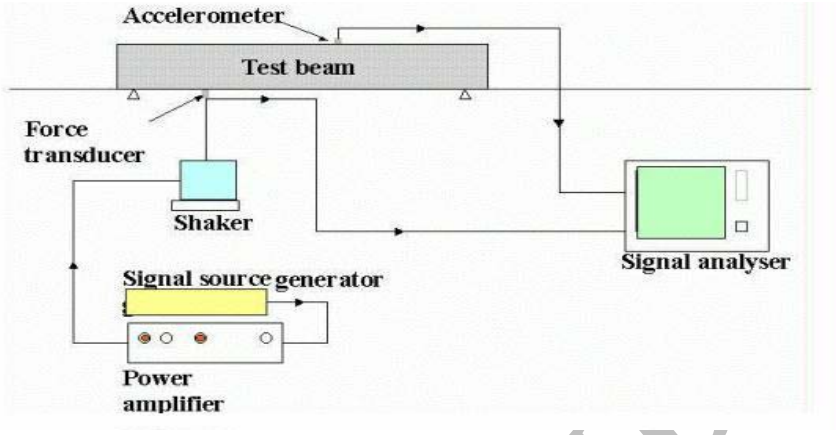

Figure 4. Modal test set-up

4.1 Crack at 0.5L

Table 2 shows that the results for flexural stiffness obtained from modal tests range from 3.4366 x 10^6 Nm^2 for an un-cracked beam with zero load to 1.8997 x 10^6 Nm^2 for a beam with 1.31 mm crack width and 43 kN loading. Corresponding results from static load tests ranged from 4.0398 x 10^6 Nm^2 to 2.8825 x 10^6 Nm^2 respectively. This showed that the results obtained from the modal tests were comparable to those obtained from static load tests. In other words it showed that the algorithm proposed gave results which were in fair agreement with the results from static load tests. The results showed that there was a corresponding loss of stiffness of up to 45% as indicated by the modal tests, and up to 29% as indicated by the load tests, in the beam with an induced crack width of 1.31 mm.

Figure 5 shows that the shape indicator plot was a straight line indicating no loss of flexural stiffness for the datum beam. For Load 1 the curve dropped slightly below the datum case; while for Load 2 the loss of flexural stiffness was more significant as evidenced by a much lower drop in the curve below the datum curve. This showed that the results for global flexural stiffness were consistent with the results of local flexural stiffness.

4.2 Crack at 0.7L

Table 3 shows that the results for flexural stiffness obtained from modal tests ranged from 4.7537 x 10^6 Nm^2 for an un-cracked beam with zero load to 4.5634 x 10^6 Nm^2 for a beam with 0.7 mm crack width and 43 kN loading. Corresponding results from static load tests ranged from 4.5367 x 10^6 Nm^2 to 4.2482 x 10^6 Nm^2 respectively. This showed that the results obtained from the modal tests were almost similar to those obtained from static load tests. This showed that the algorithm proposed gave results which were in good agreement with the results from static load tests. The results showed that there was a corresponding loss of stiffness of up to 4% as indicated by the modal tests, and up to 6% as indicated by the load tests, in the beam with an applied load of 41 kN corresponding to a crack width of 0.38 mm. The loss in stiffness was apparently very small compared to the beam with a crack at 0.5*L*.

Figure 6 also shows that the shape indicator plot was a straight line indicating no loss of

flexural stiffness for the datum beam. For Load 1 the curve rose slightly above the datum case. The increase, however, was not significant, indicating that there was very little change in the flexural stiffness due to the damage. For Load 2, Load 3 and Load 4 there was an indication of increasing loss of local flexural stiffness with increasing loads and crack widths. The global flexural stiffness results obtained above showed very little change from the datum for Load 1, Load 2 and Load 3; although the plot of local flexural stiffness did show a decrease in stiffness with increasing loads and crack widths. The overall effect on the stiffness remained insignificant. There were also inflexions shown on the curves followed by further loss of stiffness.

From the values of relative stiffness obtained, it was observed that the crack in the middle caused a greater loss in stiffness compared to a crack on the right side of mid-span, for the same level of severity induced.

Table 2. Comparison of *EI* values with crack at 0.5*L*

Load (kN)	**Ave. Crack Width (mm)**	***EI* X 10^6 (Nm^2)**		**Relative stiffness**	
		Modal Test	**Load Test**	**Modal Test**	**Load Test**
0	Un-cracked	3.4366	4.0398	1	1
25	0.08	2.7009	3.4666	0.79	0.86
43	1.31	1.8997	2.8825	0.55	0.71

Table 3. Comparison of *EI* values with crack at 0.7*L*

Load (kN)	Ave. Crack Width (mm)	*EI* X 10^6 (Nm^2)		Relative stiffness	
		Modal Test	Load Test	Modal Test	Load Test
0	Un-cracked	4.7537	4.5367	1	1
25	0.073	5.2884	4.4502	1.10	0.98
41	0.383	4.8520	4.5695	1.02	1.01
43	0.7	4.5634	4.2842	0.96	0.94

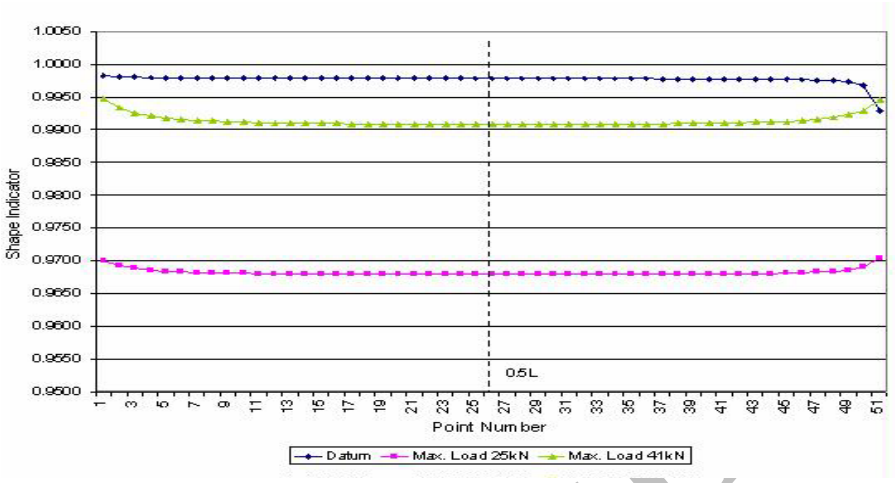

Figure 5. Normalized shape indicator for *EI* with crack at 0.5*L*

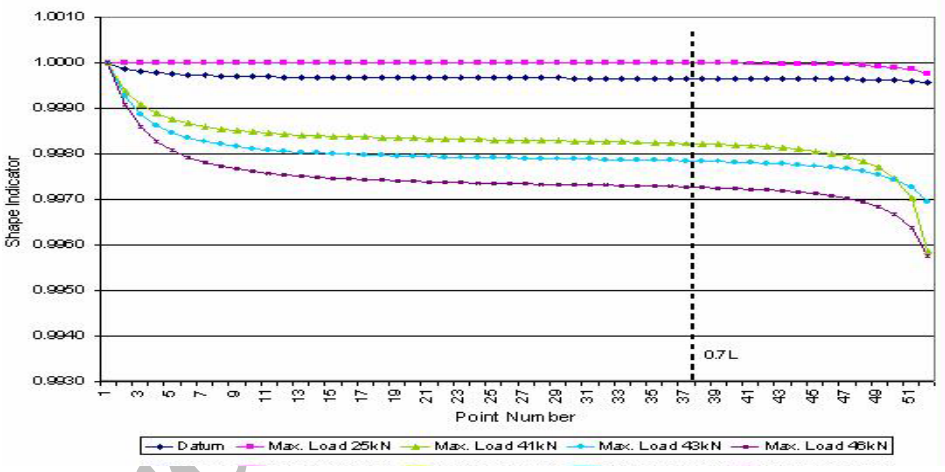

Figure 6. Normalized shape indicator for *EI* with crack at 0.7*L*

5. CONCLUSIONS

The procedure of applying curve fitting using the generalized solution model and fourth order centered finite-divided-difference to the modal data yielded the global flexural stiffness for the control and defect reinforced concrete beams. The method is in fairly good agreement with the results obtained from static load tests. The procedure is capable of indicating the presence of damage by showing a loss in the flexural stiffness. The loss of flexural stiffness is more pronounced in the case of damage in the middle than for similar extents of damage located outside the mid-span region.

REFERENCES

1. Chen, Y., Swamidas, A.S.J., Dynamic characteristics and modal parameters of a plate with a small growing surface crack, *Proc 12th International Modal Analysis Conference*, (1994) 1155-1161.
2. Dong, C., Zhang, P.Q., Feng, W.Q., and Huang, T.C., The sensitivity study of the modal parameters of a cracked beam, *Proc 12th International Modal Analysis Conference*, 1994, pp. 98-104.
3. Kam, T.Y., Lee, T.Y., Detection of cracks in structures using modal test data, *Engineering Fracture Mechanics*, No. 2, **42**(1992)381-387.
4. Lim, T.W., Structural damage detection using modal test data, *AIAA Journal*, No. 12, **29**(1991) 2271-2274.
5. Liu, P.L., Identification and damage detection of strusses using modal data, *Journal of Structural Engineering*, No. 4, **121**(1995) 599-608.
6. Narkis, Y., Identification of crack location in vibrating simply supported beams, *Journal of Sound and Vibration*, No. 4, **172**(1994) 549-558.
7. Nwosu, D.I., Swamidas, A.S.J., Guigne, J.Y., and Olowokere, D.O., Studies on influence of cracks on the dynamic response of beams, *Proc 13th International Modal Analysis Conference*, 1995, pp. 1122-1128.
8. Penny, J.E.T., Wilson, D.A.L. and Friswell M.I., Damage location in structures using vibration data, *Proc 11th International Modal Analysis Conference*, 1993, pp. 861-867.
9. Rizos, P.F., Aspragathos, N., and Dimarogonas, A.D., Identification of crack location and magnitude in a cantilever from the vibration modes, *Journal of Sound and Vibration*, No. 3, **138**(1990) 381-388.
10. Maeck, J., Abdel Wahab, M., and De Roec, G., Damage localization in reinforced concrete beams by dynamic stiffness determination, *Proc 17th International Modal Analysis Conference*, 1999, pp. 1289-1295.
11. Javor, T., Damage classification of concrete structures. the state of the art report of RILEM Technical Committee 104-DCC, *Material and Structures* **24**(1991) 253-259.
12. Konig, G. and Giegerich, G., Identification of structural properties using dynamic tests, *Proc of the IABSE Symposium on Durability of Structures*, (1989) 835-840, Lisbon.
13. Cawley, F. and Adams, R.D., The locations of defects in structures from measurements of natural frequencies, *Journal of Strain Analysis*, No. 2, **14**(1979) 49-57.
14. Friswell, M.I., Penny, J.E.T and Wilson, D.A.L., Using vibration data statistical measures to locate damage in structures, *International Journal of Analytical and Experimental Modal Analysis*, No. 4, **9**(1994) 239-254.
15. Gudmundson, P., Eigenfrequency changes of structures due to cracks, notches, or other geometrical changes, *Journal of the Mechanics and Physics of Solids*, No. 5, **30**(1982) 339-353.
16. Morassi, A., and Rovere, N., Localizing a notch in a steel frame from frequency measurements, *Journal of Engineering Mechanics-ASCE*, No. 5, **123**(1997) 422-432.
17. Casas, J.R., An experimental study on the use of dynamic tests for surveillance of concrete structures, *Materials and Structures*, **27**(1994) 588-595.
18. Salawu, O.S., and Williams, C., Damage location using vibration mode shapes, *Proc*

12th International Modal Analysis Conference, 1994, pp. 933-939.
19. West, W.M., Illustration of the use of modal assurance criterion to detect structural changes in an orbiter test specimen, *Proc. Air Force Conference on Aircraft Structural Integrity*, (1984) 1.
20. Fox, C.H.J., The location of defects in structures: a comparison of the use of natural frequency and mode shape data, *Proc 10th International Modal Analysis Conference*, 1992, pp. 522-528.
21. Ratcliffe, C.P., Damage detection using a modified Laplacian operator on mode shape data, *Journal of Sound and Vibration*, No.3, **204**(1997)505-517.
22. Pandey, A.K., Biswas, M. and Samman, M.M., Damage detection from changes in curvature mode shapes, *Journal of Sound and Vibration*, No. 2, **145**(1991) 321-332.
23. Stubbs, N., Kim, J.T. and Topole, K.G., An efficient and robust algorithm for damage localization in offshore platforms, *Proc. ASCE 10th Structures Congress*, 1992, p. 543.
24. Topole, K.G. and Stubbs, N., Nondestructive damage evaluation of a structure from limited modal parameters, *Earthquake Engineering and Structural Dynamics,* No. 11, **24**(1995) 1427-1436.
25. Topole, K.G. and Stubbs, N., Nondestructive damage evaluation in complex structures from a minimum of modal parameters, *International Journal of Analytical and Experimental Modal Analysis*, No.2, **10**(1995) 95-103.
26. Stubbs, N. and Kim, J.T., Damage localization in structures without baseline modal parameters, *AIAA Journal*, No.8, **34**(1996) 1644-1649.
27. Chance, J., Tomlinson, G.R. and Worden, K., Simplified approach to the numerical and experimental modeling of the dynamics of a cracked beam, *Proc. 12thInternational Modal Analysis Conference,* 1994, p. 778.
28. Shahrivar, F. and Bouwkamp, J.G., Damage detection in offshore platforms using vibration information, *Journal of Energy Resources Technology* **108**(1986) 97-106.
29. Altay, G.A. and Dokmeci, M.C. Comments. *International Journal of Solids and Structures*. **40**(18) (2003) 4699-4706.
30. Transforms and nonlinear regression - User's Manual, Jandel Scientific Software, United States, 1995.
31. SigmaStat - User's Manual, Jandel Scientific Software, United States, 1995.

Appendix A

Table A.1. Characteristics of loading cycles for beam with crack at 0.5*L*

	Label	**Maximum Load Applied**	**Note**
No load	Datum	0 kN	Undamaged
Load cycle 1	ML25	24.4 kN	First crack occurred
Load cycle 2	ML43	43.2 kN	Crack developed extensively
Final load cycle	Failure	54.6 kN	Loaded until fail

Table A.2. Characteristics of loading cycles for beam with crack at 0.7*L*

	Label	**Maximum Load Applied**	**Note**
No load	Datum	0 kN	Undamaged
Load cycle 1	ML25	24.64 kN	First crack occurred
Load cycle 2	ML41	41.36 kN	Crack developed extensively
Load cycle 3	ML43	42.97 kN	Crack developed extensively

Appendix B

Table B.1. History of stiffness determination for beam with crack at 0.5*L*

	Label	**Maximum Load Applied**	**Stiffness Determination from Load Test**
No load	Datum	0 kN	
Load cycle 1	ML25	24.4 kN	Datum
Load cycle 2	ML43	43.2 kN	Load cycle 1
Final load cycle	Failure	54.6 kN	Load cycle 2

Table B.2. History of stiffness determination for beam with crack at 0.7*L*

	Label	**Maximum Load Applied**	**Stiffness Determination from Load Test**
No load	Datum	0 kN	
Load cycle 1	ML25	24.64 kN	Datum
Load cycle 2	ML41	41.36 kN	Load cycle 1
Load cycle 3	ML43	42.97 kN	Load cycle 2
Load cycle 4	ML46	46.31 kN	Load cycle 3